

Investigation of the semileptonic transition of the B into the orbitally excited charmed tensor meson

K. Azizi¹ *, H. Sundu² †, S. Şahin² ‡

¹ Department of Physics, Doğuş University, Acıbadem-Kadıköy, 34722 Istanbul, Turkey

² Department of Physics , Kocaeli University, 41380 Izmit, Turkey

Abstract

The transition form factors of the semileptonic $B \rightarrow D_2^*(2460)\ell\bar{\nu}$ ($\ell = \tau, \mu, e$) decay channel are calculated within the framework of the three-point QCD sum rules. The fit functions of the form factors are then used to estimate the total decay width and branching ratio of this transition. The order of branching ratio shows that this channel can be detected at LHCb.

PACS number(s): 11.55.Hx, 13.20.He, 14.40.Lb

*e-mail: kazizi@dogus.edu.tr

†e-mail: hayriye.sundu@kocaeli.edu.tr

‡e-mail: 095131004@kocaeli.edu.tr

1 Introduction

As it is well known, the semileptonic decays of B meson are very promising tools in constraining the standard model parameters, determination of the elements of the Cabibbo-Kobayashi-Maskawa (CKM) matrix, understanding the origin of the CP violation and looking for new physics effects. Over the last few years, the radially excited charmed mesons have been in the focus of much attention both theoretically and experimentally. In 2010, BaBar Collaboration reported their isolation of a number of orbitally excited charmed mesons [1]. This report has stimulated the theoretical works devoted to the semileptonic decays of B meson into the orbitally excited charmed meson (for instance see [2–5] and references therein). As the decays of B meson into orbitally excited charmed mesons can provide a substantial contribution to the total semileptonic decay width, such processes deserve more detailed studies. Moreover, a better knowledge on these transitions can help us in the analysis of signals and backgrounds of inclusive and exclusive decays of b -hadrons.

In this article, we calculate the transition form factors of the semileptonic decays of $B \rightarrow D_2^*(2460)\ell\bar{\nu}$ in the framework of the three-point QCD sum rules. This approach is one of the attractive and applicable nonperturbative tools to hadron physics based on the QCD Lagrangian [6]. As the $D_2^*(2460)$ is a tensor meson containing derivatives in its interpolating current, we start our calculations in the coordinate space then we apply the Fourier transformation to go to the momentum space. Based on the general philosophy of the method, to suppress the contributions of the higher states and continuum, we finally apply the Borel transformation and continuum subtraction which bring some auxiliary parameters whose working regions are determined demanding some criteria. The transition form factors are then used to calculate the decay width and branching ratio of the semileptonic decay channel under consideration.

The BaBar Collaboration has recently measured the ratios for the branching fractions of the B to charmed pseudoscalar D and vector D^* mesons at τ channel to those of the e and μ channels [7]. The obtained results deviate at the level of 3.4σ from the existing theoretical predictions in SM [7, 8]. Hence, there is a possibility that the semileptonic transitions containing heavy b and c quarks and the τ lepton are bring out the effects of particles with large couplings to the heavier fermions [9]. Determination of these ratios of the branching fractions in B to charmed tensor D_2^* channel can also be important from this point of view whether these anomalous in the pseudoscalar and vector channels exist in the tensor channel or not. We will be able to answer this question when having the experimental data in this channel. By the aforementioned experimental progress on the identification and spectroscopy of the orbitally excited charmed mesons as well as the developments at LHC and by considering the orders of the branching ratios in the tensor channel, we hope it will be possible in near future.

This article is arranged as follows. We derive the QCD sum rules for the form factors defining the semileptonic $B \rightarrow D_2^*(2460)\ell\bar{\nu}$ transition in section 2. The last section is devoted to the numerical analysis of the form factors, calculations of the branching ratios of the transition under consideration at different lepton channels as well as our concluding remarks.

2 QCD sum rules for transition form factors of $B \rightarrow D_2^*(2460)\ell\bar{\nu}$

This section is dedicated to calculation of the form factors of the $B \rightarrow D_2^*(2460)\ell\bar{\nu}$ transition applying the QCD sum rules technique. The starting point is to consider the following tree-point correlation function:

$$\Pi_{\mu\alpha\beta}(q^2) = i^2 \int d^4x \int d^4y e^{-ip \cdot x} e^{ip' \cdot y} \langle 0 | \mathcal{T} [J_{\alpha\beta}^{D_2^*}(y) J_\mu^{tr}(0) J^{B\dagger}(x)] | 0 \rangle, \quad (1)$$

where, \mathcal{T} is the time ordering operator and $J_\mu^{tr}(0) = \bar{c}(0)\gamma_\mu(1 - \gamma_5)b(0)$ is the transition current. Also, the interpolating current of the B and $D_2^*(2460)$ mesons are written in terms of the quark fields as

$$J^B(x) = \bar{u}(x)\gamma_5 b(x) \quad (2)$$

$$J_{\alpha\beta}^{D_2^*}(y) = \frac{i}{2} \left[\bar{u}(y)\gamma_\alpha \overleftrightarrow{\mathcal{D}}_\beta(y)c(y) + \bar{u}(y)\gamma_\beta \overleftrightarrow{\mathcal{D}}_\alpha(y)c(y) \right], \quad (3)$$

where the $\overleftrightarrow{\mathcal{D}}_\beta(y)$ denotes the four-derivative with respect to y acting on the left and right, simultaneously and is given as

$$\overleftrightarrow{\mathcal{D}}_\beta(y) = \frac{1}{2} \left[\overrightarrow{\mathcal{D}}_\beta(y) - \overleftarrow{\mathcal{D}}_\beta(y) \right], \quad (4)$$

with,

$$\begin{aligned} \overrightarrow{\mathcal{D}}_\beta(y) &= \overrightarrow{\partial}_\beta(y) - i\frac{g}{2}\lambda^a A_\beta^a(y), \\ \overleftarrow{\mathcal{D}}_\beta(y) &= \overleftarrow{\partial}_\beta(y) + i\frac{g}{2}\lambda^a A_\beta^a(y), \end{aligned} \quad (5)$$

where, λ^a are the Gell-Mann matrices and $A_\beta^a(x)$ is the external gluon fields. These fields are expressed in terms of the gluon field strength tensor, using the Fock-Schwinger gauge ($x^\beta A_\beta^a(y) = 0$),

$$A_\beta^a(y) = \int_0^1 d\alpha \alpha y_\nu G_{\nu\beta}^a(\alpha y) = \frac{1}{2}y_\nu G_{\nu\beta}^a(0) + \frac{1}{3}y_\eta y_\nu \mathcal{D}_\eta G_{\nu\beta}^a(0) + \dots \quad (6)$$

Following the general idea of the QCD sum rule approach, the aforementioned correlation function is calculated via two different ways: once in terms of hadronic degrees of freedom called phenomenological or physical side and, the second, in terms of QCD degrees of freedom called theoretical or QCD side. By matching these two representations, the QCD sum rules for the form factors are obtained. To stamp down the contributions of the higher states and continuum, we will apply double Borel transformation with respect to the momentum squared of the initial and final states and will use the quark-hadron duality assumption.

2.1 The phenomenological side

On the phenomenological side, the correlation function is obtained inserting two complete sets of intermediate states with the same quantum numbers as the interpolating currents J^B and $J^{D_2^*}$ into Eq. (1). After performing four-integrals over x and y , we get

$$\Pi_{\mu\alpha\beta}^{phen}(q^2) = \frac{\langle 0 | J_{\alpha\beta}^{D_2^*}(0) | D_2^*(p', \epsilon) \rangle \langle D_2^*(p', \epsilon) | J_\mu^{tr}(0) | B(p) \rangle \langle B(p) | J_B^\dagger(0) | 0 \rangle}{(p^2 - m_B^2)(p'^2 - m_{D_2^*(2460)}^2)} + \dots, \quad (7)$$

where \dots represents contributions of the higher states and continuum, and ϵ is the polarization tensor of the $D_2^*(2460)$ tensor meson. To proceed, we need to define the following matrix elements in terms of decay constants and form factors:

$$\begin{aligned} \langle 0 | J_{\alpha\beta}^{D_2^*}(0) | D_2^*(p', \epsilon) \rangle &= m_{D_2^*}^3 f_{D_2^*} \epsilon_{\alpha\beta} \\ \langle B(p) | J_B^\dagger(0) | 0 \rangle &= -i \frac{f_B m_B^2}{m_u + m_b} \\ \langle D_2^*(p', \epsilon) | J_\mu^{tr}(0) | B(p) \rangle &= h(q^2) \varepsilon_{\mu\nu\lambda\eta} \epsilon^{*\nu\theta} P_\theta P^\lambda q_\eta - i K(q^2) \epsilon_{\mu\nu}^* P^\nu \\ &\quad - i \epsilon_{\lambda\eta}^* P^\lambda P^\eta [P_\mu b_+(q^2) + q_\mu b_-(q^2)], \end{aligned} \quad (8)$$

where $h(q^2)$, $K(q^2)$, $b_+(q^2)$ and $b_-(q^2)$ are transition form factors; and $f_{D_2^*}$ and f_B are leptonic decay constants of D_2^* and B mesons, respectively. By combining Eqs. (7) and (8) and performing summation over polarization tensors using

$$\epsilon_{\alpha\beta} \epsilon_{\nu\theta}^* = \frac{1}{2} T_{\alpha\nu} T_{\beta\theta} + \frac{1}{2} T_{\alpha\theta} T_{\beta\nu} - \frac{1}{3} T_{\alpha\beta} T_{\nu\theta}, \quad (9)$$

with

$$T_{\alpha\nu} = -g_{\alpha\nu} + \frac{p'_\alpha p'_\nu}{m_{D_2^*(2460)}^2}, \quad (10)$$

the final representation of the physical side is obtained as

$$\begin{aligned} \Pi_{\mu\alpha\beta}^{phen} &= \frac{f_{D_2^*} f_B m_{D_2^*} m_B^2}{8(m_b + m_u)(p^2 - m_B^2)(p'^2 - m_{D_2^*}^2)} \left\{ \frac{2}{3} \left[-\Delta K(q^2) + \Delta' b_-(q^2) \right] q_\mu g_{\beta\alpha} \right. \\ &\quad + \frac{2}{3} \left[(\Delta - 4m_{D_2^*}^2) K(q^2) + \Delta' b_+(q^2) \right] P_\mu g_{\beta\alpha} + i(\Delta - 4m_{D_2^*}^2) h(q^2) \varepsilon_{\lambda\nu\beta\mu} P_\lambda P_\alpha q_\nu \\ &\quad \left. + \Delta K(q^2) q_\alpha g_{\beta\mu} + \text{other structures} \right\} + \dots, \end{aligned} \quad (11)$$

where

$$\begin{aligned} \Delta &= m_B^2 + 3m_{D_2^*(2460)}^2 - q^2, \\ \Delta' &= m_B^4 - 2m_B^2(m_{D_2^*(2460)}^2 + q^2) + (m_{D_2^*(2460)}^2 - q^2)^2. \end{aligned} \quad (12)$$

We will use the explicitly written structures to find the aforesaid form factors.

2.2 The QCD side

On the QCD side, the correlation function is calculated by expanding the time ordering product of the B and $D_2^*(2460)$ mesons' currents and the transition current via operator product expansion (OPE) in deep Euclidean region where the short (perturbative) and long distance (nonperturbative) contributions are separated. By inserting the previously represented currents into Eq. (1) and after contracting out all quark fields applying the Wick's theorem, we obtain

$$\begin{aligned} \Pi_{\mu\alpha\beta}^{QCD}(q^2) &= \frac{-i^3}{4} \int d^4x \int d^4y e^{-ip \cdot x} e^{ip' \cdot y} \\ &\times \left\{ Tr \left[S_u^{ik}(x-y) \gamma_\alpha \overleftrightarrow{D}_\beta(y) S_c^{ij}(y) \gamma_\mu (1-\gamma_5) S_b(-x)^{jk} \gamma_5 \right] + [\beta \leftrightarrow \alpha] \right\}. \end{aligned} \quad (13)$$

To proceed, we need the expressions of the heavy and light quarks propagators. Up to the terms considered in this study they are respectively given as

$$S_Q^{ij}(x) = \frac{i}{(2\pi)^4} \int d^4k e^{-ik \cdot x} \left\{ \frac{\not{k} + m_c}{k^2 - m_c^2} \delta_{ij} + \dots \right\}, \quad (14)$$

and

$$S_q^{ij}(x) = i \frac{\not{x}}{2\pi^2 x^4} \delta_{ij} - \frac{m_q}{4\pi^2 x^2} \delta_{ij} - \frac{\langle \bar{q}q \rangle}{12} \left(1 - i \frac{m_q}{4} \not{x} \right) \delta_{ij} - \frac{x^2}{192} m_0^2 \langle \bar{q}q \rangle \left(1 - i \frac{m_q}{6} \not{x} \right) \delta_{ij} + \dots. \quad (15)$$

After putting the expressions of the quarks propagators and applying the derivatives with respect to x and y in Eq. (13), the following expression for the QCD side of the correlation function in coordinate space is obtained:

$$\begin{aligned} \Pi_{\mu\alpha\beta}^{QCD}(q^2) &= \frac{i^5 N_c}{4} \int \frac{d^4k}{(2\pi)^4} \int \frac{d^4k_1}{(2\pi)^4} \int d^4x e^{-ip \cdot x} \int d^4y e^{ip' \cdot y} \frac{e^{-ik \cdot y}}{k^2 - m_c^2} \frac{e^{ik_1 \cdot x}}{k_1^2 - m_b^2} \left\{ ik_\beta \right. \\ &\times Tr \left[\left(\frac{i(\not{x} - \not{y})}{2\pi^2 (x-y)^4} - \frac{\langle \bar{u}u \rangle}{12} - \frac{(x-y)^2}{192} m_0^2 \langle \bar{u}u \rangle \right) \gamma_\alpha (\not{k} + m_c) \gamma_\mu (1-\gamma_5) (\not{k}_1 + m_b) \gamma_5 \right] \\ &+ Tr \left[\left(\frac{i}{2\pi^2} \left(\frac{4(x-y)_\beta (\not{x} - \not{y})}{(x-y)^6} - \frac{\gamma_\beta}{(x-y)^4} \right) + \frac{(x-y)_\beta}{96} m_0^2 \langle \bar{u}u \rangle \right) \gamma_\alpha (\not{k} + m_c) \gamma_\mu \right. \\ &\times \left. \left. (1-\gamma_5) (\not{k}_1 + m_b) \gamma_5 \right] + [\beta \leftrightarrow \alpha] \right\}, \end{aligned} \quad (16)$$

where $N_c = 3$ is the color factor. In order to perform the integrals, first the terms containing $\frac{1}{((x-y)^2)^n}$ are transformed to the momentum space ($(x-y) \rightarrow t$), then the replacements $x_\mu \rightarrow i \frac{\partial}{\partial p_\mu}$ and $y_\mu \rightarrow -i \frac{\partial}{\partial p'_\mu}$ are made. The four-integrals over x and y give us two Dirac Delta functions which help us perform the four-integrals over k and k_1 . The last four-integral over t is performed using the Feynman parametrization and

$$\int d^4t \frac{(t^2)^\beta}{(t^2 + L)^\alpha} = \frac{i\pi^2 (-1)^{\beta-\alpha} \Gamma(\beta+2) \Gamma(\alpha-\beta-2)}{\Gamma(2) \Gamma(\alpha) [-L]^{\alpha-\beta-2}}. \quad (17)$$

As a result, the QCD side of the correlation function is obtained in terms of the corresponding structures as

$$\begin{aligned}\Pi_{\mu\alpha\beta}^{QCD}(q^2) &= \left(\Pi_1^{pert}(q^2) + \Pi_1^{nonpert}(q^2)\right)q_\alpha g_{\beta\mu} + \left(\Pi_2^{pert}(q^2) + \Pi_2^{nonpert}(q^2)\right)q_\mu g_{\beta\alpha} \\ &+ \left(\Pi_3^{pert}(q^2) + \Pi_3^{nonpert}(q^2)\right)P_\mu g_{\beta\alpha} + \left(\Pi_4^{pert}(q^2) + \Pi_4^{nonpert}(q^2)\right)\varepsilon_{\lambda\nu\beta\mu}P_\lambda P_\alpha q_\nu \\ &+ \text{other structures},\end{aligned}\quad (18)$$

where, the perturbative parts $\Pi_i^{pert}(q^2)$ are given in terms of double dispersion integrals as

$$\Pi_i^{pert}(q^2) = \int ds \int ds' \frac{\rho_i(s, s', q^2)}{(s - p^2)(s' - p'^2)}. \quad (19)$$

The spectral densities $\rho_i(s, s', q^2)$ are given by the imaginary parts of the $\Pi_i^{pert}(q^2)$ functions, i.e., $\rho_i(s, s', q^2) = \frac{1}{\pi} \text{Im}[\Pi_i^{pert}(q^2)]$. After lengthy calculations the spectral densities corresponding to the selected structures are obtained as

$$\begin{aligned}\rho_1(s, s', q^2) &= \int_0^1 dx \int_0^{1-x} dy \left\{ \frac{1}{64\pi^2(x+y-1)^3} \left[m_b(x+y-1)^3(8x^2 - 8y^2 + 6x - 6y - 6) \right. \right. \\ &+ 3m_c(8x^5 + 6x^4(4y-3) - 6x(y-1)^2(3+2y+4y^2) - 2(2+3y+4y^2) \\ &\times (y-1)^3 + 2x^3(1-18y+8y^2) + x^2(22-5y-16y^3)) \left. \right] \Big\}, \\ \rho_2(s, s', q^2) &= \int_0^1 dx \int_0^{1-x} dy \left\{ \frac{-1}{32\pi^2(x+y-1)^3} \left[m_b(x+y-1)^3(2x^2 - 2y^2 + 6x - 6y - 3) \right. \right. \\ &+ 3m_c(2x^5 - 3x(y-1)^2(1+2y^2) - (y-1)^3(1+2y^2) + x^3(5-12y+4y^2) \\ &+ 6x^4(y-1) + x^2(1+4y-4y^3)) \left. \right] \Big\}, \\ \rho_3(s, s', q^2) &= \int_0^1 dx \int_0^{1-x} dy \left\{ \frac{1}{32\pi^2(x+y-1)^3} \left[m_b(2x^2 + 2y^2 + x(6+4y) + 6y-3) \right. \right. \\ &\times (x+y-1)^3 + 3m_c(2x^5 + 2x^4(5y-3) + (y-1)^3(1+2y^2) + x(y-1)^2 \\ &\times (3-4y+10y^2) + x^3(7-24y+20y^2) + x^2(20y^3-36y^2+20y-5)) \left. \right] \Big\}, \\ \rho_4(s, s', q^2) &= 0.\end{aligned}\quad (20)$$

For the nonperturbative parts we get

$$\begin{aligned}\Pi_1^{nonpert}(q^2) &= \left\{ \frac{m_b^4 + 4m_b^2 m_c^2 + 2m_b^2(m_c^2 - q^2) + (m_c^2 - q^2)^2}{64r^2 r'^2} + \frac{m_b^2 m_c^2(m_b^2 + m_c^2 - q^2)}{32r^2 r'^3} \right. \\ &+ \frac{m_b^3 m_c + m_b^2 m_c^2 + 2m_b m_c^3 + m_c^4 - m_c^2 q^2}{32r r'^3} - \frac{m_b^2 + 4m_b m_c + m_c^2 - q^2}{64r r'^2} \\ &+ \frac{m_b^4 + 2m_b^3 m_c + m_b^2 m_c^2 - m_b^2 q^2}{32r^3 r'} + \frac{3m_b^2 + 2m_b m_c + 3m_c^2 - 3q^2}{64r^2 r'} + \frac{m_b^2}{32r^3} \Big\}\end{aligned}$$

$$\begin{aligned}
& + \left\{ \frac{m_c^2}{32r'^3} - \frac{1}{32r'^2} + \frac{1}{32r^2} - \frac{1}{32rr'} \right\} m_0^2 \langle \bar{u}u \rangle \\
& - \left(\frac{m_b^2 + 2m_b m_c + m_c^2 - q^2}{16rr'} + \frac{1}{16r} + \frac{1}{16r'} \right) \langle \bar{u}u \rangle, \\
\Pi_2^{nonpert}(q^2) &= 0, \\
\Pi_3^{nonpert}(q^2) &= \frac{m_0^2 \langle \bar{u}u \rangle}{8rr'}, \\
\Pi_4^{nonpert}(q^2) &= -i \left\{ \frac{m_c^2}{32rr'^3} + \frac{m_b^2}{32r^3 r'} + \frac{m_b^2 + m_c^2 - q^2}{64r^2 r'^2} - \frac{1}{32r^2 r'} \right\} m_0^2 \langle \bar{u}u \rangle + i \frac{\langle \bar{u}u \rangle}{16rr'}. \quad (21)
\end{aligned}$$

where $r = p^2 - m_b^2$ and $r' = p'^2 - m_c^2$.

To obtain sum rules for the form factors, the coefficients of the same structures from both sides of the correlation functions are matched. In order to suppress the contributions of the higher states and continuum, we apply double Borel transformation with respect to the initial and final momenta squared using

$$\widehat{B} \frac{1}{(p^2 - m_b^2)^m} \frac{1}{(p'^2 - m_c^2)^n} \rightarrow \frac{(-1)^{m+n}}{\Gamma[m]\Gamma[n]} e^{-m_b^2/M^2} e^{-m_c^2/M'^2} \frac{1}{(M^2)^{m-1} (M'^2)^{n-1}}, \quad (22)$$

where M^2 and M'^2 are Borel mass parameters. We also use the quark-hadron duality assumption, i.e.,

$$\rho^{higher \text{ states}}(s, s', q^2) = \rho^{OPE}(s, s', q^2) \theta(s - s_0) \theta(s' - s'_0), \quad (23)$$

where s_0 and s'_0 are continuum thresholds in the initial and final mesonic channels, respectively. After these procedures, the following sum rules for the form factors are obtained:

$$\begin{aligned}
K(q^2) &= \frac{8(m_b + m_u)}{f_B f_{D_2^*} m_{D_2^*} (m_B^2 q^2 - m_B^4 - 3m_B^2 m_{D_2^*}^2)} e^{\frac{m_B^2}{M^2}} e^{\frac{m_{D_2^*}^2}{M'^2}} \\
&\left\{ \int_{(m_b+m_u)^2}^{s_0} ds \int_{(m_c+m_u)^2}^{s'_0} ds' \int_0^1 dx \int_0^{1-x} dy e^{\frac{-s}{M^2}} e^{\frac{-s'}{M'^2}} \left[\frac{1}{256\pi^4 (x+y-1)^3} \right. \right. \\
&\left. \left(2m_b(x+y-1)^3(4x^2 - 4y^2 + 3x - 3y - 3) + 3m_c(8x^5 + 6x^4(4y-3) \right. \right. \\
&- 6x(y-1)^2(3+2y+4y^2) - 2(y-1)^3(2+3y+4y^2) + 2x^3(1-18y+8y^2) \\
&+ \left. \left. x^2(22-5y-16y^3) \right) \right] \theta[L(s, s', q^2)] + e^{\frac{-m_B^2}{M^2}} e^{\frac{-m_{D_2^*}^2}{M'^2}} \left[\frac{\langle \bar{u}u \rangle}{16} (m_b^2 + 2m_b m_c + m_c^2 - q^2) \right. \\
&+ \frac{m_0^2 \langle \bar{u}u \rangle}{64} \left(2 + \frac{3m_b^2 + 2m_b m_c + 3m_c^2 - 3q^2}{M^2} - \frac{m_b^2 + 4m_b m_c + m_c^2 - q^2}{M'^2} \right. \\
&- \frac{m_b^4 + 2m_b^3 m_c + m_b^2 m_c^2 - m_b^2 q^2}{M^4} - \frac{m_b^3 m_c + m_b^2 m_c^2 + 2m_b m_c^3 + m_c^4 - m_c^2 q^2}{M'^4} \\
&- \left. \left. \frac{m_b^4 + 4m_b m_c^3 + 2m_b^2 m_c^2 + m_c^4 - m_c^2 q^2 - m_b^2 q^2 + q^4}{M^2 M'^2} + \frac{m_b^5 m_c + m_b m_c^5 - m_b^2 m_c^2 q^2}{M^2 M'^4} \right) \right] \Big\}, \\
b_-(q^2) &= - \frac{12(m_b + m_u)}{f_B f_{D_2^*} m_B^2 m_{D_2^*} (m_B^4 + (m_{D_2^*}^2 - q^2)^2 - 2m_B^2 (m_{D_2^*}^2 + q^2))} e^{\frac{m_B^2}{M^2}} e^{\frac{m_{D_2^*}^2}{M'^2}}
\end{aligned}$$

$$\begin{aligned}
& \times \left\{ \int_{(m_b+m_u)^2}^{s_0} ds \int_{(m_c+m_u)^2}^{s'_0} ds' \int_0^1 dx \int_0^{1-x} dy e^{\frac{-s}{M^2}} e^{\frac{-s'}{M'^2}} \left[\frac{1}{128\pi^4(x+y-1)^3} \right. \right. \\
& \times \left(m_b(x+y-1)^3(3-6x-2x^2+6y+2y^2) - 3m_c \left(6x^4(y-1) - 3x(y-1)^2(1+2y^2) \right. \right. \\
& - \left. \left. (y-1)^3(1+2y^2) + x^3(5-12y+4y^2) + x^2(1+4y-4y^3) + 2x^5 \right) \right] \theta[L(s, s', q^2)] \\
& - \left. e^{\frac{-m_B^2}{M^2}} e^{\frac{-m_{D_2^*}^2}{M'^2}} \frac{f_B f_{D_2^*} m_B^2 m_{D_2^*} (m_B^2 + 3m_{D_2^*}^2 + q^2)}{12(m_b + m_u)} K(q^2) \right\}, \\
b_+(q^2) &= - \frac{12(m_b + m_u)}{f_B f_{D_2^*} m_B^2 m_{D_2^*} (m_B^4 + (m_{D_2^*}^2 - q^2)^2 - 2m_B^2(m_{D_2^*}^2 + q^2))} e^{\frac{m_B^2}{M^2}} e^{\frac{m_{D_2^*}^2}{M'^2}} \\
& \times \left\{ \int_{(m_b+m_u)^2}^{s_0} ds \int_{(m_c+m_u)^2}^{s'_0} ds' \int_0^1 dx \int_0^{1-x} dy e^{\frac{-s}{M^2}} e^{\frac{-s'}{M'^2}} \left[\frac{1}{128\pi^4(x+y-1)^3} \right. \right. \\
& \times \left(m_b(x+y-1)^3(2x^2+2y^2+6x+6y+4xy-3) + 3m_c \left(2x^5 - 6x^4 + 10x^4y \right. \right. \\
& + \left. \left. (y-1)^3(1+2y^2) + x(y-1)^2(3-4y+10y^2) + x^2(20y^3 - 36y^2 + 20y - 5) \right. \right. \\
& + \left. \left. x^3(7-24y+20y^2) \right) \right] \theta[L(s, s', q^2)] - \frac{m_0^2 \langle \bar{u}u \rangle}{8} e^{\frac{-m_b^2}{M^2}} e^{\frac{-m_c^2}{M'^2}} \\
& - \left. e^{\frac{-m_B^2}{M^2}} e^{\frac{-m_{D_2^*}^2}{M'^2}} \frac{f_B f_{D_2^*} m_B^2 m_{D_2^*} (m_{D_2^*}^2 - m_B^2 + q^2)}{12(m_b + m_u)} K(q^2) \right\}, \\
h(q^2) &= \frac{8(m_b + m_u)}{f_B f_{D_2^*} m_B^2 m_{D_2^*} (m_{D_2^*}^2 - m_B^2 + q^2)} e^{\frac{m_B^2}{M^2}} e^{\frac{m_{D_2^*}^2}{M'^2}} e^{\frac{-m_b^2}{M^2}} e^{\frac{-m_c^2}{M'^2}} \left\{ - \frac{\langle \bar{u}u \rangle}{16} \right. \\
& + \left. \frac{m_0^2 \langle \bar{u}u \rangle}{64} \left[\frac{2}{M^2} + \frac{2}{M'^2} + \frac{m_b^2}{M^4} + \frac{m_c^2}{M'^4} + \frac{m_b^2 - m_c^2 + q^2}{M^2 M'^2} \right] \right\}, \tag{24}
\end{aligned}$$

where

$$L(s, s', q^2) = s'x - s'x^2 - m_c^2x - m_b^2y + sy + q^2xy - sxy - s'xy - sy^2. \tag{25}$$

3 Numerical results and discussions

In this part, we numerically analyze the obtained sum rules for the form factors in the previous section and obtain their variations in terms of q^2 . For this aim we need some input parameters whose values are given in Table 1. Besides these input parameters, the sum rules for the form factors contain four auxiliary parameters, namely the Borel mass parameters M^2 and M'^2 and continuum thresholds s_0 and s'_0 . We shall find their working regions such that the form factors weakly depend on these parameters. The continuum thresholds are not completely arbitrary but they are related to the energy of the first excited state in initial and final mesonic channels. Our calculations show that in the intervals $31 \text{ GeV}^2 \leq s_0 \leq 35 \text{ GeV}^2$ and $7 \text{ GeV}^2 \leq s'_0 \leq 9 \text{ GeV}^2$, our results weakly depend on the continuum thresholds. The working regions for the Borel mass parameters are determined by requiring that not only the contributions of the higher states and continuum are sufficiently suppressed but also the

Parameters	Values
m_c	$(1.275 \pm 0.025) \text{ GeV}$
m_b	$(4.65 \pm 0.03) \text{ GeV}$
m_e	0.00051 GeV
m_μ	0.1056 GeV
m_τ	1.776 GeV
$m_{D_2^*(2460)}$	$(2.4626 \pm 0.0007) \text{ GeV}$
m_B	$(5.27925 \pm 0.00017) \text{ GeV}$
f_B	$(210 \pm 40) \text{ MeV}$
$f_{D_2^*(2460)}$	0.0317 ± 0.0092
G_F	$1.17 \times 10^{-5} \text{ GeV}^{-2}$
V_{cb}	$(41.2 \pm 1.1) \times 10^{-3}$
$\langle 0 \bar{u}u(1\text{GeV}) 0 \rangle$	$-(0.24 \pm 0.01)^3 \text{ GeV}^3$
$m_0^2(1\text{GeV})$	$(0.8 \pm 0.2) \text{ GeV}^2$
τ_B	$(1641 \pm 8) \times 10^{-15} \text{ s}$

Table 1: Input parameters used in calculations [10–14].

contributions of the operators with higher dimensions are relatively small, i.e., the series of sum rules for the form factors are convergent. As a result, we find the working regions $10 \text{ GeV}^2 \leq M^2 \leq 20 \text{ GeV}^2$ and $5 \text{ GeV}^2 \leq M'^2 \leq 15 \text{ GeV}^2$. To show how the form factors depend on the auxiliary parameters, as examples, we depict the variations of the form factors $K(q^2)$ and $b_+(q^2)$ at $q^2 = 0$ with respect to the variations of the related auxiliary parameters in their working regions in figures 1 and 2. From these figures, we see that the form factors weakly depend on the auxiliary parameters in their working regions.

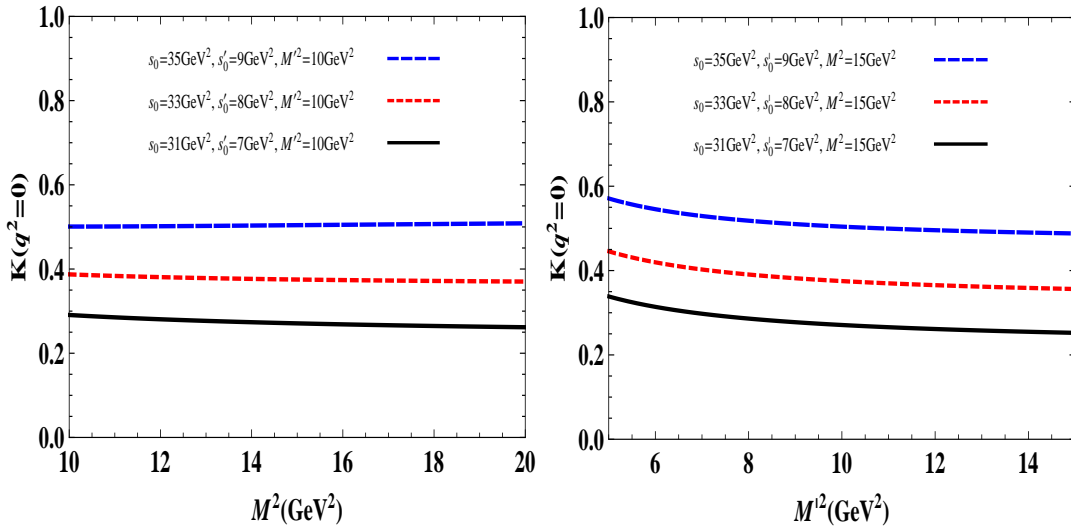


Figure 1: **Left:** $K(q^2 = 0)$ as a function of the Borel mass M^2 at fixed values of the s_0 , s'_0 and M^2 . **Right:** $K(q^2 = 0)$ as a function of the Borel mass M'^2 at fixed values of the s_0 , s'_0 and M^2 .

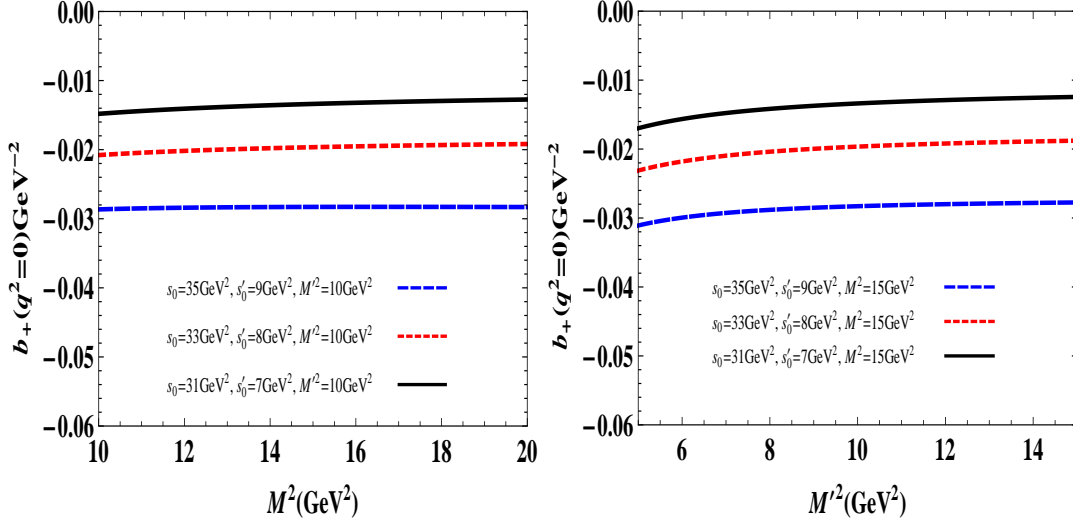


Figure 2: **Left:** $b_+(q^2 = 0)$ as a function of the Borel mass M^2 at fixed values of the s_0 , s'_0 and M'^2 . **Right:** $b_+(q^2 = 0)$ as a function of the Borel mass M'^2 at fixed values of the s_0 , s'_0 and M^2 .

	f_0	c_1	c_2	m_{fit}^2
$K(q^2)$	0.54 ± 0.14	0.70 ± 0.07	0.41 ± 0.02	27.88 ± 0.01
$b_-(q^2)$	$0.007 \pm 0.002 \text{ GeV}^{-2}$	0.14 ± 0.04	10.70 ± 0.82	27.88 ± 0.01
$b_+(q^2)$	$-0.03 \pm 0.01 \text{ GeV}^{-2}$	1.20 ± 0.15	22.52 ± 1.68	27.88 ± 0.01
$h(q^2)$	$-0.010 \pm 0.003 \text{ GeV}^{-2}$	1.19 ± 0.13	1.12 ± 0.08	27.88 ± 0.01

Table 2: Parameters appearing in the fit function 1 of the form factors.

Using the working regions for the continuum thresholds and Borel mass parameters as well as other input parameters we proceed to find the behavior of the form factors in terms of q^2 . Our calculations show that the form factors are truncated at $q^2 \simeq 5\text{GeV}^2$. In order to estimate the decay width of the $B \rightarrow D_2^*(2460)\ell\bar{\nu}$ transition, we have to obtain their fit functions in the whole physical region, $m_\ell^2 \leq q^2 \leq (m_B - m_{D_2^*})^2$. We find that the sum rules predictions for the form factors are well fitted to the following function:

$$f(q^2) = f_0 \exp \left[c_1 \frac{q^2}{m_{fit}^2} + c_2 \left(\frac{q^2}{m_{fit}^2} \right)^2 \right] \quad (26)$$

where, the values of the parameters f_0 , c_1 , c_2 and m_{fit}^2 are presented in Table 2. In the following, we will recall this parametrization as *fit function 1*. To compare our results with other parametrization, we also use the following fit functions to extrapolate the form factors to whole physical regions (see [15–18]):

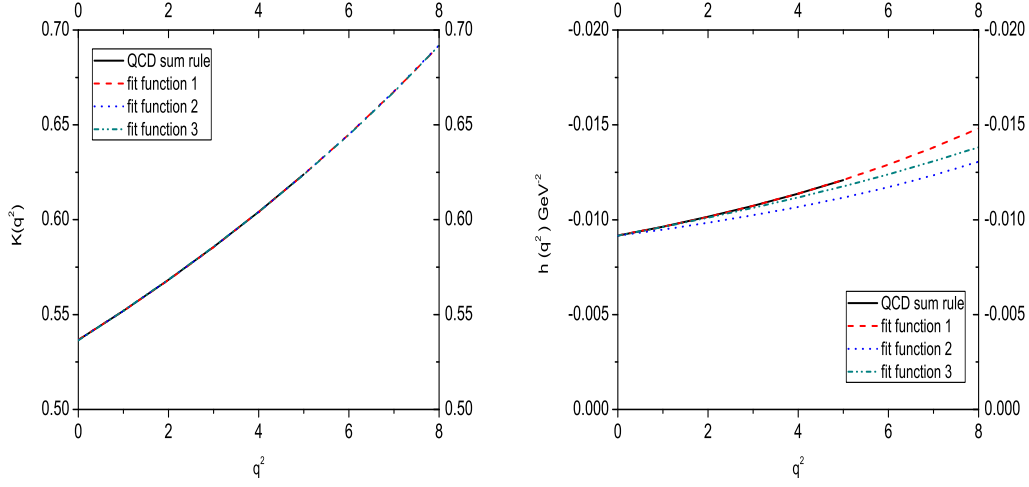


Figure 3: **Left:** $K(q^2)$ as a function of q^2 at $M^2 = 15\text{GeV}^2$, $M'^2 = 10\text{GeV}^2$, $s_0 = 35\text{GeV}^2$ and $s'_0 = 9\text{GeV}^2$. **Right:** $h(q^2)$ as a function of q^2 at $M^2 = 15\text{GeV}^2$, $M'^2 = 10\text{GeV}^2$, $s_0 = 35\text{GeV}^2$ and $s'_0 = 9\text{GeV}^2$.

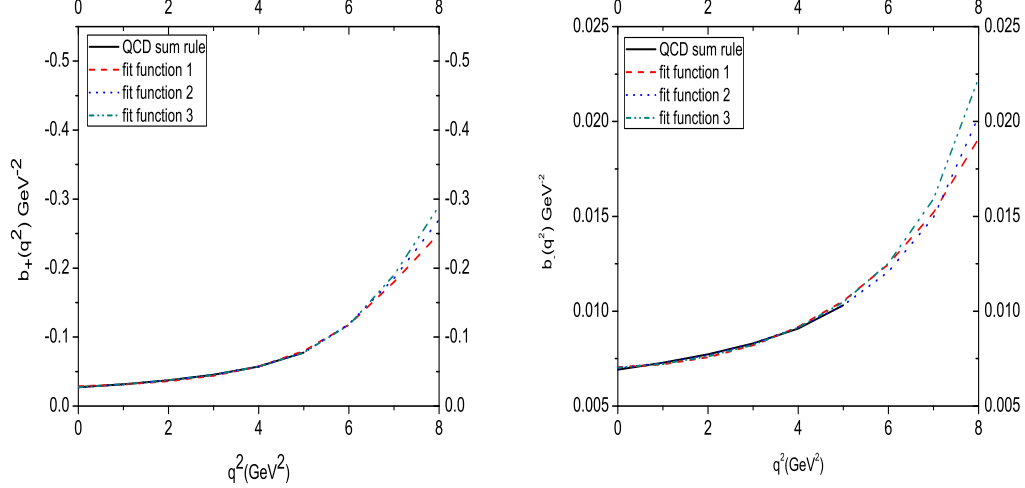


Figure 4: **Left:** $b_+(q^2)$ as a function of q^2 at $M^2 = 15\text{GeV}^2$, $M'^2 = 10\text{GeV}^2$, $s_0 = 35\text{GeV}^2$ and $s'_0 = 9\text{GeV}^2$. **Right:** $b_-(q^2)$ as a function of q^2 at $M^2 = 15\text{GeV}^2$, $M'^2 = 10\text{GeV}^2$, $s_0 = 35\text{GeV}^2$ and $s'_0 = 9\text{GeV}^2$.

- *fit function 2*

$$f(q^2) = \frac{f_0}{1 - a(\frac{q^2}{m_B^2}) + b(\frac{q^2}{m_B^2})^2}, \quad (27)$$

- *fit function 3*

$$f(q^2) = \frac{f_0}{\left(1 - \frac{q^2}{m_B^2}\right) \left[1 - A\left(\frac{q^2}{m_B^2}\right) + B\left(\frac{q^2}{m_B^2}\right)^2\right]}, \quad (28)$$

where the parameters a , b , A and B and the values of corresponding form factors at $q^2 = 0$ are given in Tables 3 and 4, respectively.

	f_0	a	b
$K(q^2)$	0.54 ± 0.14	0.75 ± 0.03	-0.014 ± 0.006
$b_-(q^2)$	$0.007 \pm 0.002 \text{ GeV}^{-2}$	0.95 ± 0.04	-3.14 ± 1.34
$b_+(q^2)$	$-0.03 \pm 0.01 \text{ GeV}^{-2}$	1.41 ± 0.06	-4.63 ± 2.05
$h(q^2)$	$-0.010 \pm 0.003 \text{ GeV}^{-2}$	1.27 ± 0.05	0.058 ± 0.002

Table 3: Parameters appearing in the fit function 2 of the form factors.

	f_0	A	B
$K(q^2)$	0.54 ± 0.14	-0.15 ± 0.06	0.31 ± 0.03
$b_-(q^2)$	$0.007 \pm 0.002 \text{ GeV}^{-2}$	-0.36 ± 0.16	-7.72 ± 0.86
$b_+(q^2)$	$-0.03 \pm 0.01 \text{ GeV}^{-2}$	1.89 ± 0.81	-2.39 ± 0.27
$h(q^2)$	$-0.010 \pm 0.003 \text{ GeV}^{-2}$	0.25 ± 0.10	-0.35 ± 0.04

Table 4: Parameters appearing in the fit function 3 of the form factors.

The dependences of form factors on q^2 at different fixed values of auxiliary parameters are depicted in figures 3 and 4. These figures include the sum rules results (up to the truncated point) as well as the results obtained using the above mentioned three different fit functions. From these figures it is clear that, in the case of the form factors $K(q^2)$, $b_+(q^2)$ and $b_-(q^2)$, all three fit functions reproduce the sum rules results up to the truncated point, however, we see small differences between the predictions of these fit functions at higher values of q^2 except for the form factor $K(q^2)$ that all fit functions give the same results. In the case of the form factor $h(q^2)$, the parametrization 1 well fits to the sum rule result, but we see considerable differences of prediction of this parametrization with those of fit functions 2 and 3, especially at higher values of q^2 .

Now we proceed to calculate the decay width and branching ratio of the process under consideration. The differential decay width for $B \rightarrow D_2^*(2460)\ell\bar{\nu}$ transition is obtained as

[19]

$$\begin{aligned}
\frac{d\Gamma}{dq^2} = & \frac{\lambda(m_B^2, m_{D_2^*}^2, q^2)}{4m_{D_2^*}^2} \left(\frac{q^2 - m_\ell^2}{q^2} \right)^2 \frac{\sqrt{\lambda(m_B^2, m_{D_2^*}^2, q^2)} G_F^2 V_{cb}^2}{384m_B^3 \pi^3} \left\{ \frac{1}{2q^2} \left[3m_\ell^2 \lambda(m_B^2, m_{D_2^*}^2, q^2) [V_0(q^2)]^2 \right. \right. \\
& + (m_\ell^2 + 2q^2) \left| \frac{1}{2m_{D_2^*}} \left[(m_B^2 - m_{D_2^*}^2 - q^2)(m_B - m_{D_2^*}) V_1(q^2) - \frac{\lambda(m_B^2, m_{D_2^*}^2, q^2)}{m_B - m_{D_2^*}} V_2(q^2) \right] \right|^2 \Big] \\
& + \frac{2}{3} (m_\ell^2 + 2q^2) \lambda(m_B^2, m_{D_2^*}^2, q^2) \left[\left| \frac{A(q^2)}{m_B - m_{D_2^*}} - \frac{(m_B - m_{D_2^*}) V_1(q^2)}{\sqrt{\lambda(m_B^2, m_{D_2^*}^2, q^2)}} \right|^2 \right. \\
& \left. \left. + \left| \frac{A(q^2)}{m_B - m_{D_2^*}} + \frac{(m_B - m_{D_2^*}) V_1(q^2)}{\sqrt{\lambda(m_B^2, m_{D_2^*}^2, q^2)}} \right|^2 \right] \right\}, \tag{29}
\end{aligned}$$

where

$$\begin{aligned}
A(q^2) &= -(m_B - m_{D_2^*}) h(q^2), \\
V_1(q^2) &= -\frac{K(q^2)}{m_B - m_{D_2^*}}, \\
V_2(q^2) &= (m_B - m_{D_2^*}) b_+(q^2), \\
V_0(q^2) &= \frac{m_B - m_{D_2^*}}{2m_{D_2^*}} V_1(q^2) - \frac{m_B + m_{D_2^*}}{2m_{D_2^*}} V_2(q^2) - \frac{q^2}{2m_{D_2^*}} b_-(q^2), \\
\lambda(a, b, c) &= a^2 + b^2 + c^2 - 2ab - 2ac - 2bc. \tag{30}
\end{aligned}$$

After performing integration over q^2 in Eq. (29) in the interval $m_\ell^2 \leq q^2 \leq (m_B - m_{D_2^*})^2$, we obtain the total decay widths and branching ratios for all leptons and three different fit functions presented in Table 5. The errors in the results belong to the uncertainties in determination of the working regions for the auxiliary parameters as well as errors in the other input parameters. From this Table, it is clear that, for the e and μ channels, all fit functions give roughly the same results. In the case of τ , the fit functions 2 and 3 have approximately the same predictions, but they give results roughly %38 smaller than that of the fit function 1. As it is expected, the values for the branching ratios in the cases of e and μ are very close to each other for all fit functions. The orders of branching fractions show that this transition can be detected at LHCb for all lepton channels. Note that there are experimental data on the products of branching fractions for the decay chain $\mathcal{B}(B \rightarrow D_2^* \ell \bar{\nu}) \mathcal{B}(D_2^* \rightarrow D\pi)$ provided by Belle [20] and BaBar [21, 22] Collaborations:

$$\begin{aligned}
\mathcal{B}(B^+ \rightarrow \bar{D}_2^* \ell'^+ \bar{\nu}_{\ell'}) \mathcal{B}(\bar{D}_2^* \rightarrow D\pi) &= 2.2 \pm 0.3 \pm 0.4 & \text{Belle [20],} \\
\mathcal{B}(B^+ \rightarrow \bar{D}_2^* \ell'^+ \bar{\nu}_{\ell'}) \mathcal{B}(\bar{D}_2^* \rightarrow D\pi) &= 1.4 \pm 0.2 \pm 0.2 & \text{BaBar [21, 22].} \tag{31}
\end{aligned}$$

where $\ell' = e$ or μ . Considering the recent experimental progress especially at LHC we hope we will have experimental data on the branching fraction of the semileptonic $B \rightarrow D_2^*(2460) \ell \bar{\nu}$ transition in near future, comparison of which with the results of the present work can give more information about the nature and internal structure of the $D_2^*(2460)$ tensor meson.

fit function 1	$\Gamma(GeV)$	Br
$B \rightarrow D_2^*(2460)\tau\bar{\nu}_\tau$	$(6.52 \pm 2.20) \times 10^{-17}$	$(0.16 \pm 0.06) \times 10^{-3}$
$B \rightarrow D_2^*(2460)\mu\bar{\nu}_\mu$	$(4.04 \pm 1.18) \times 10^{-16}$	$(1.00 \pm 0.29) \times 10^{-3}$
$B \rightarrow D_2^*(2460)e\bar{\nu}_e$	$(4.05 \pm 1.19) \times 10^{-16}$	$(1.01 \pm 0.30) \times 10^{-3}$
fit function 2	$\Gamma(GeV)$	Br
$B \rightarrow D_2^*(2460)\tau\bar{\nu}_\tau$	$(4.09 \pm 1.28) \times 10^{-17}$	$(0.10 \pm 0.03) \times 10^{-3}$
$B \rightarrow D_2^*(2460)\mu\bar{\nu}_\mu$	$(4.06 \pm 1.26) \times 10^{-16}$	$(1.01 \pm 0.32) \times 10^{-3}$
$B \rightarrow D_2^*(2460)e\bar{\nu}_e$	$(4.08 \pm 1.28) \times 10^{-16}$	$(1.02 \pm 0.32) \times 10^{-3}$
fit function 3	$\Gamma(GeV)$	Br
$B \rightarrow D_2^*(2460)\tau\bar{\nu}_\tau$	$(4.80 \pm 1.60) \times 10^{-17}$	$(0.12 \pm 0.04) \times 10^{-3}$
$B \rightarrow D_2^*(2460)\mu\bar{\nu}_\mu$	$(4.18 \pm 1.32) \times 10^{-16}$	$(1.04 \pm 0.34) \times 10^{-3}$
$B \rightarrow D_2^*(2460)e\bar{\nu}_e$	$(4.20 \pm 1.32) \times 10^{-16}$	$(1.05 \pm 0.34) \times 10^{-3}$

Table 5: Numerical results for the decay widths and branching ratios at different lepton channels for different fit functions.

At the end of this section we would like to calculate the ratio of the branching fraction in the case of τ to that of the e or μ . From our calculations we obtain that

$$\mathcal{R} = \frac{B \rightarrow D_2^*(2460)\tau\bar{\nu}_\tau}{B \rightarrow D_2^*(2460)\ell'\bar{\nu}_{\ell'}} = \begin{cases} 0.16 \pm 0.04 & \text{fit function 1,} \\ 0.10 \pm 0.02 & \text{fit function 2,} \\ 0.11 \pm 0.02 & \text{fit function 3.} \end{cases} \quad (32)$$

As we previously mentioned the SM predictions in the B to pseudoscalar and vector charmed mesons deviate at the level of 3.4σ from the experimental data. Our result on \mathcal{R} in the case of tensor charmed current can be checked in future experiments. Comparison of the experimental data with the result of this work will illustrate whether these anomalous in the pseudoscalar and vector channels exist also in the tensor channel or not.

References

- [1] P. del Amo Sanchez et al. [BABAR Collaboration], Phys. Rev. D 82, 111101 (2010).
- [2] D. Becirevic, B. Blossier, A. Gerardin, A. Le Yaouanc, F. Sanfilippo, arXiv:1301.7336 [hep-ph].
- [3] J. Segovia, C. Albertus, D.R. Entem, F. Fernandez, E. Hernandez, M.A. Perez-Garcia, Phys. Rev. D 84, 094029 (2011).

- [4] F. De Fazio, PoS HQL2012, 001 (2012).
- [5] P. Colangelo, F. De Fazio, F. Giannuzzi and S. Nicotri, Phys. Rev. D 86, 054024 (2012).
- [6] M. A. Shifman, A. I. Vainshtein and V. I. Zakharov, Nucl. Phys. B 147, 385 (1979).
- [7] J. P. Lees et al. [BaBar Collaboration], Phys. Rev. Lett. 109, 101802 (2012).
- [8] S. Fajfer, J. F. Kamenik and I. Nisandzic, Phys. Rev. D 85, 094025 (2012).
- [9] P. Biancospino, P. Colangelo, F. De Fazio, arXiv:1302.1042 [hep-ph].
- [10] J. Beringer et al., (Particle Data Group) Phys. Rev. D 86, 010001, (2012).
- [11] H. Sundu, K. Azizi, Eur. Phys. J. A 48 (2012) 81.
- [12] H. Na, C. J. Monahan, C. T. H. Davies, R. Horgan, G. P. Lepage, J. Shigemitsu, Phys. Rev. D 86, (2012) 034506.
- [13] B. L. Ioffe, Prog. Part. Nucl. Phys. 56, 232 (2006).
- [14] H. G. Dosch, M. Jamin and S. Narison, Phys. Lett. B 220, 251 (1989); V. M. Belyaev, B. L. Ioffe, Sov. Phys. JETP, 57, 716 (1982).
- [15] W. Wang, Phys. Rev. D 83, 014008 (2011).
- [16] R.-H. Li, C.-D. Lü, W. Wang, Phys. Rev. D 83, 034034 (2011).
- [17] C.-D. Lü, W. Wang, Phys. Rev. D 85, 034014 (2012).
- [18] H.-Y. Cheng, C.-K. Chua, C.-W. Hwang, Phys. Rev. D 69, 074025 (2004).
- [19] X.-X. Wang, W. Wang and C.-D. Lü, Phys. Rev. D 79, 114018, (2009).
- [20] D. Liventsev et al. (Belle Collaboration), Phys. Rev. D 77, 091503 (2008).
- [21] B. Aubert et al. (BaBar Collaboration), Phys. Rev. Lett. 101, 261802 (2008).
- [22] B. Aubert et al. (BaBar Collaboration), Phys. Rev. Lett. 103, 051803 (2009).